



5-2014

Solute Additives and Neutron Absorber Alloys for the Improvement of Spent Fuel Pool Safety and Increased Storage Space

Seth H. Jobe
sjobe1@utk.edu

John R. Chalmers

Zach Hensley

Austin O'Connor

Nathan Shoman

See next page for additional authors

Follow this and additional works at: https://trace.tennessee.edu/utk_chanhonoproj

 Part of the [Nuclear Engineering Commons](#)

Recommended Citation

Jobe, Seth H.; Chalmers, John R.; Hensley, Zach; O'Connor, Austin; Shoman, Nathan; and Weeks, Matthew, "Solute Additives and Neutron Absorber Alloys for the Improvement of Spent Fuel Pool Safety and Increased Storage Space" (2014). *Chancellor's Honors Program Projects*.
https://trace.tennessee.edu/utk_chanhonoproj/1744

This Dissertation/Thesis is brought to you for free and open access by the Supervised Undergraduate Student Research and Creative Work at TRACE: Tennessee Research and Creative Exchange. It has been accepted for inclusion in Chancellor's Honors Program Projects by an authorized administrator of TRACE: Tennessee Research and Creative Exchange. For more information, please contact trace@utk.edu.

Author

Seth H. Jobe, John R. Chalmers, Zach Hensley, Austin O'Connor, Nathan Shoman, and Matthew Weeks

Solute Additives and Neutron Absorber Alloys for the Improvement of Spent Fuel Pool Safety and Increased Storage Space

J.R. Chalmers
Zach Hensley
Seth Jobe
Austin O'Connor
Nathan Shoman
Matthew Weeks

April 25, 2014
System Design Draft Report

Table of Contents

1. Abstract.....	4
2. Introduction.....	5
2.1 Background.....	5
3. Spent Fuel Pool Additive.....	9
3.1 Introduction and Motivation.....	9
3.2 Positive Effects of SFP Additive.....	10
3.2a Grace-Period Extension.....	11
3.2b Effects on Concrete Underlying Pools.....	12
3.3 Negative Effects of SFP Additive.....	12
3.3a Thermal-Hydraulic Concerns.....	13
3.3b Corrosion Concerns.....	14
4. Neutron Absorber Alloy.....	17
4.1 Introduction and Motivation.....	17
4.2 Alloy Melting Experiments.....	17
4.2a Experimental Equipment.....	17
4.2b Experiment 1: Cu-Cd.....	18
4.2c Experiment 2: Ag45 Alloy.....	19
4.3 Criticality Safety Analysis.....	21
4.3a Standard Spent Fuel Model.....	22
4.3b Spent Fuel Pool with Close-Packed Bundles.....	23
4.3c Spent Fuel Pool with Rod Spacing Removed.....	24
4.4 Thermal Analysis.....	25
4.5 Neutron Activation Analysis.....	30
5. Conclusions.....	33
5.1 Spent Fuel Pool Additive.....	33
5.2 Neutron Absorber Alloy.....	33
6. Future Work.....	36
6.1 Additive Concerns.....	36

6.2 Thermal Analysis	37
6.3 Economic Viability and Retrofit Potential.....	37
7. References.....	39
Appendix A: SCALE 6.1 Models	41
Appendix B: MATLAB Thermal Modeling Code.....	47

List of Figures

Figure 1: Nuclear facilities in the United States exceeding fuel pool capacity [1].....	6
Figure 2: Chemical hood, furnace, and melting pot used in our experiments (L to R)	18
Figure 3: Ceramic crucible containing oxidized cadmium and copper	19
Figure 4: Zircaloy tubing samples after Ag45 dip application	20
Figure 5: Corner of SFP with 6-mm spacing between bundles	22
Figure 6: k_{eff} versus Ag-45 coating thickness for a standard SFP	23
Figure 7: Corner of SFP with minimal bundle spacing	24
Figure 8: Close-up comparison of tight-packed array with and without Ag45 alloy	25
Figure 9: Cross section of a fuel pellet after exposure to irradiation and thermal stresses.....	27
Figure 10: Effect on pellet-to-cladding gap distance on thermal conductivity.....	28
Figure 11: Projected outer fuel-clad temperature as a function of alloy coating thickness	29

1. Abstract

This report covers two separate design studies on improving the safety and storage configuration of spent nuclear fuel pools. The first study set out to find a chemical additive for spent fuel pools that would raise the boiling point such that the risk of rapid boil off is reduced in an extended loss-of-power accident scenario. This study is conducted in response to concerns raised early in the 2011 Fukushima Daiichi accident that spent fuel pools could have boiled away, causing damage to spent fuel assemblies. Sodium acetate was found to be a strong candidate since it is not hazardous to plant personnel or the environment while exhibiting acceptable corrosive characteristics on the timescale expected for SFP storage.

The second study has been conducted to determine the effectiveness and feasibility of adding a neutron poison coating to spent nuclear fuel assemblies to reduce criticality concerns in a scenario where compact storage configurations are desired. Brazing experiments found that a 45% Ag, 15% Cu, 16% Zn, and 24% Cd (by weight) alloy will successfully wet to zirconium. Criticality safety performance of the alloy was evaluated with the SCALE 6.1 software package which showed that the alloy could safely act as the sole neutron poison in a greatly condensed storage configuration. Thermal impact of the coating is also considered and a rough calculation is provided with a suggestion for future work. Neutron activation in the alloy is also analyzed and it is noted that the transmutation of silver into cadmium may be significant due to the high silver content.

2. Introduction

2.1 Background

Commercial nuclear power plants in the United States do not include reprocessing as a part of the nuclear fuel cycle. With the possibility of Yucca Mountain as a long-term nuclear waste repository no longer available, nuclear plants are forced to keep their waste on site. Spent fuel pools and dry casks are the main forms of storage for the used fuel assemblies. The spent fuel pools maintain sub-criticality, cooling, and shielding. Dry casks usually just provide cooling capabilities and radiation shielding, as criticality is no longer a concern by the time assemblies are put in the casks.

Used fuel removed from the core of a reactor is first placed in a spent fuel pool. Spent fuel pools are large concrete basins lined with stainless steel. BWRs typically have elevated spent fuel pools in secondary containment so that the top of the pool is located on the same level as the refueling floor. PWRs use ground level spent fuel pools located in buildings outside of the reactor building and must transfer the used fuel assemblies through a transfer tube. On average, used fuel spends about five years in a spent fuel pool before being moved into dry cask storage.

In the United States, there is currently no off-site storage for used fuel. This is causing many nuclear facilities to exceed their spent fuel capacity. **Figure 1** contains data [1] from the Nuclear Energy Institute (NEI), illustrating that this problem and how it will continue to get worse in the near future.

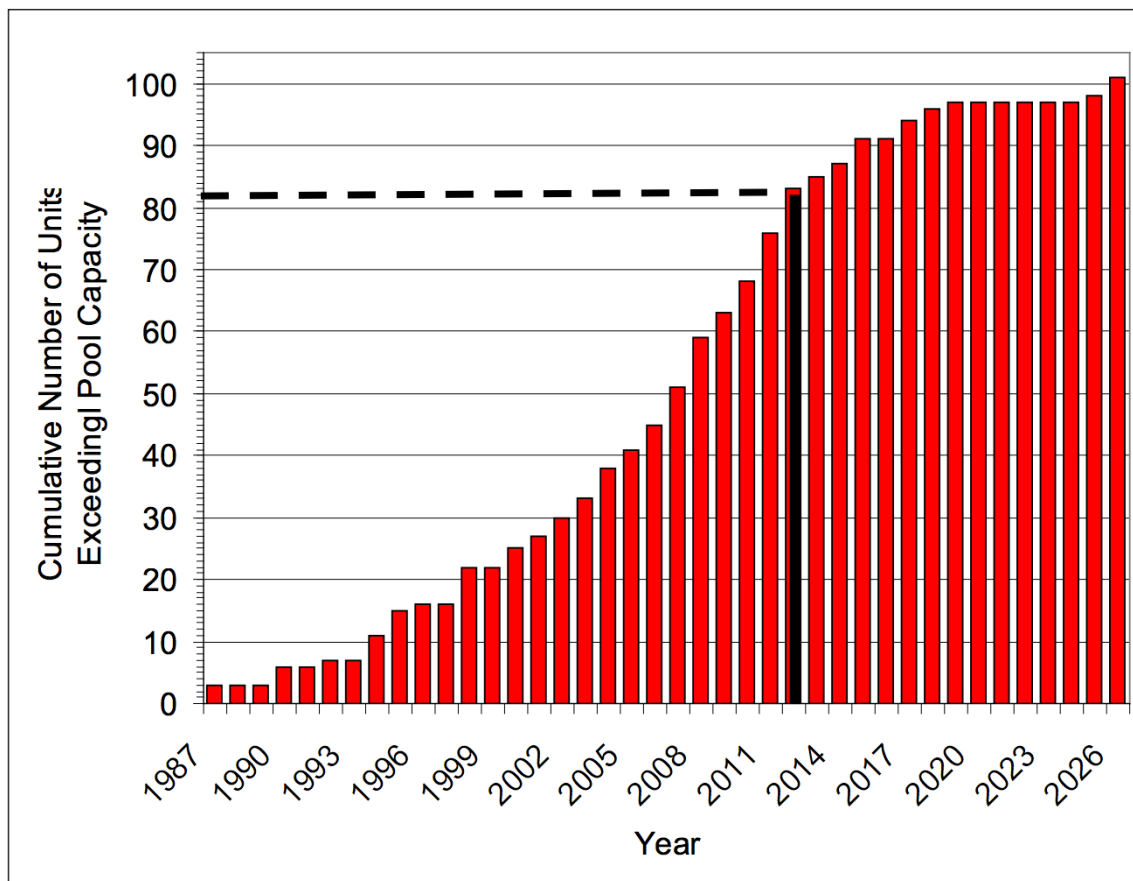


Figure 1: Nuclear facilities in the United States exceeding fuel pool capacity [1]

This diagram shows that over eighty of the reactor units in the United States have exceeded their fuel pool capacity, and that by 2026, all operating units the US will have reached full capacity. As facilities continue to add more fuel assemblies to their pools, they have had to add more neutron absorbing materials. Many facilities began using Boraflex absorbers, a boron based neutron poison in silicone rubber. However, the silicone was degraded by γ -irradiation, leading to complications in spent fuel pools. The failure of this material costs these companies large amounts of money to replace it with another material and clean the pools of degraded material. Maintaining sub-criticality in pools with an ever-increasing amount of fuel assemblies remains a key topic in the field of waste management following the natural disaster that eventually caused

a loss of all power to cooling systems at the Fukushima Daiichi plant in Japan. This loss of cooling caused the water in Unit 4 of the plant to start boiling off, but the used fuel assemblies were never uncovered or reached dangerous temperatures. However, this occurrence created a large push for emergency passive cooling systems since it was a matter of time before fuel rods became uncovered and damaged, potentially releasing highly radioactive fission products to the environment.

2.2 Project Goals

The first objective of the design project is to examine potential additives to spent fuel pool water that would raise the boiling point of the water. This would allow more time before the water would start to boil in an emergency situation. Unfortunately, the water composition of spent fuel pools is strictly regulated. The spent fuel pool water is the same water from the reactors cores themselves. This means that pure H₂O is desired with a small concentration of boron additive used in PWR designs. Any substance added to the water could not be corrosive to the zircaloy fuel pins or any important primary coolant system components. However, we feel that there may be a nitrate or acetate that will significantly raise the boiling point of the water and not have a negative effect on the water composition.

The main goal of the project is to develop a neutron poison alloy that can coat individual fuel rods in the assemblies in hopes of making it safe to use more compact spent fuel storage configurations. Our plan is to braze an alloy with a known neutron poison to the fuel assemblies in a dip coating process. A brazed alloy would provide a thin but effective absorber layer to help maintain sub-criticality. This coating would also be a neutron absorber that would not degrade significantly during irradiation.

When looking for a potential alloy, we will be looking for alloys with a eutectic point (melting temperature) at a temperature that does not exceed the Nuclear Regulatory Commission's (NRC) maximum temperatures for fuel pins, for both in the fuel pools and dry casks [2]. The maximum clad temperature for fuel pins in a pool is around 570 ° C and around 400° C in a dry cask. Two potential alloys we have selected include a cadmium-copper alloy and a cadmium-copper-silver-zinc alloy. Both of these alloys have eutectic melting points between 500 and 600 °C. Once one of our alloys has wetted the zircaloy fuel assemblies, we hope the neutron absorption effect from the coating will allow for the removal of current neutron absorber plates in the fuel pools. This will potentially allow for more space in the fuel pools for additional assemblies. This could also allow for more fuel assemblies to be packed into individual dry cask containers. We will perform criticality simulations using the SCALE¹ codes to confirm the effect that they alloy will have on criticality safety. We will also need to perform heat transfer calculations to confirm that the added layer of the alloy does not reduce heat transfer and pose a meltdown risk.

¹ Available from the Radiation Safety Information Computational Center (RSICC) at Oak Ridge National Laboratory

3. Spent Fuel Pool Additive

3.1 Introduction and Motivation

The events following the 2011 Tohoku Earthquake included destruction of the means of decay heat removal of the spent fuel pools (SFP) [3]. While the accident did not result in damage to stored fuel assemblies, a similar accident could result in damage to fuel assemblies and subsequent radiological release to the environment. The typical loading of the spent fuel pools of operating light water reactors entails potentially catastrophic consequences in the event that loss of cooling is not mitigated in the event of an accident. We propose the addition of a soluble compound to the spent fuel pool of a nuclear reactor under accident conditions, in the event that continued access to the SFP is endangered or lost. The addition of a soluble additive to the pool water will raise the boiling point of the pool, permitting an extension of the typical grace period and a reduction in the probability of fuel damage.

In the event of a sustained loss of SFP cooling, the SFP pool water enthalpy continually rises, leading to boiling in the fuel racks and evaporative loss of the pool water inventory. Eventually, enough volume is lost that two-phase water cooling of the fuel is removed. For shrouded boiling water reactor fuel, the loss of cooling first occurs for the lower-burnup assemblies. This seemingly paradoxical phenomenon is due to the fact that the thermal power of the lower (submerged) portion of the fuel assembly drives a two-phase cooling flow through the top (uncovered) of the fuel assembly. Lower thermal power results in less swell and earlier removal of two-phase cooling. Earlier removal of two-phase cooling results in earlier elevation of the fuel cladding to dangerous temperatures. Conversely, partially submerged fuel assemblies with higher thermal power generation will be able to sustain effective cooling for the top of the

assembly for longer as the SFP water levels lower in an accident. Once the cladding temperature reaches a sufficiently high value, the zirconium will oxidize in a steam atmosphere at a rate sufficient to cause ignition and sustainment of an exothermic reaction which will destroy the cladding and result in relocation (such as violent expulsion, melting, or other forms of fuel deformation and release) of contained fuel and fission products to the atmosphere. Relocation of fuel may occur along with relocation of installed SFP neutron absorber elements, but it is possible that relocation could result in criticality, either during pool boiling, or following re-introduction of coolant. For example, if fuel were to melt away from absorbers, it could form a concentrated geometry and achieve critical conditions that may be exacerbated by neutron moderation from water, leading to unexpected complications. Cladding failures, with or without a subsequent criticality accident, would result in large releases of fission products to the environment and significant consequences to the public.

3.2 Positive Effects of SFP Additive

The addition of a sodium acetate soluble additive to the pool water is proposed in order to extend the grace period for all negative consequences following the failure of the spent fuel pool cooling system. The mechanism by which the additive does this is the elevation of the boiling point of the pool water due to the colligative effects of a solute in aqueous solution. Elevation of the boiling point would have positive effects on both the SFP heat removal rate, and the heat capacity of the pool. The heat removal rate of the SFP will improve over baseline once the bulk temperature of the pool exceeds the typical boiling point of normal pool water, due to increased heat transfer to the liner and surrounding concrete. The heat capacity is improved by raising the upper temperature limit of the pool water.

3.2a Grace-Period Extension

Due to the higher temperatures at the interfaces between the pool and liner, and the pool and atmosphere, higher ambient heat removal is expected. The heat of dissolution of the crystalline product (energy is absorbed during melting and can be released by recrystallization), the increased heat transfer at higher endpoint temperatures, and the increased heat capacity will all act to increase the grace period for all negative consequences of loss of pool water inventory. A 10°C increase in boiling point would result in a 15% increased time to boiling for the initial pool temperature of 35°C (as was the case at Fukushima). For the Fukushima plant with the highest SFP thermal load, Unit 4, this would extend the time to boiling from 40 hours to 46 hours. This calculation assumes that the spent fuel pool has been sloshed due to seismic acceleration down to 11m depth. If this grace period is pro-rated for consideration of the logistics of long-range transport of technical accident response equipment (perhaps due to catastrophic local conditions at a reactor), then the relative extension of the time that emergency response personnel have to install and initiate additional equipment is even further extended. For example, if the time until boiling in an extended loss-of-power accident is 40 hours for a typical SFP, and the initial 20 hours are reserved for preparing emergency response equipment (leaving 20 hours for hands-on emergency work), then an additive that extends time to boil-off by ~5 hours is effectively extending the actual execution time available to emergency responders by 25% (25 hours versus the original 20 hours) despite appearing to only be a 12.5% increase in response time (45 hours versus the original 40 hours). Extension of this rule to the prediction of evaporation uncovering the top of active fuel and beyond requires detailed analysis, including consideration of the character and properties of the solution as it is concentrated by evaporation,

along with the expected surface condition of the upper region of the fuel assemblies as acetate deposits accumulate on non-wetted surfaces.

3.2b Effects on Concrete Underlying Pools

Research by Al Otoom, et al., [4] indicates that external treatment of concrete with aqueous sodium acetate solutions significantly reduces the permeability of the concrete to water. Treatment of a 20 wt. % solution provides the optimal reduction in permeability. This effect could mitigate the migration of fission products to groundwater in the event of a beyond-design basis accident (DBA) which causes failure of the pool liner and small cracks in the concrete supporting structure. This research also found improvement of the mechanical properties of concrete within the range of concentrations expected to be useful for nuclear purposes.

3.3 Negative Effects of SFP Additive

Addition of large amounts of a solid crystalline additive complicates thermal-hydraulic analysis of SFP behavior under accident conditions [4], and poses corrosion challenges during the period of time that the pool contains a significant concentration of additive. While Sodium Acetate is capable of storing significant energy after cooling from a supersaturated condition, we expect that the turbulent conditions of a SFP being recovered from a significant heat up will force crystallization during cooling and prevent the formation of a significant stored energy source. The process of sodium acetate recrystallization is exothermic so a large amount of previously absorbed energy could be unexpectedly released back into the pool water if a supersaturated condition was achieved and then lost to an undesired recrystallization event. This effect could be of substantial concern if an emergency response plan relied on the formation of a heavily supersaturated sodium acetate solution. While the addition to the pool could be

controlled so as to prevent saturation at the time of addition, excessive water loss could result in a supersaturated condition if turbulence, as produced by boiling, was not sufficient to begin crystallization. Additionally, a system which slowly and continuously added crystalline sodium acetate to the pool would introduce sufficient seed crystals to prevent supersaturation during pool cooldown.

3.3a Thermal-Hydraulic Concerns

Addition of large amounts of additive while the pool water is at low temperature could result in occlusion of the rack inlet holes, preventing cyclic flow of cooling water through the fuel assembly. This situation could be mitigated by either titrating addition, or delaying addition until pool temperature is sufficiently high to permit rapid dissolution of additive inventory beyond the maximum amount which will not occlude flow through the fuel assemblies. Addition once the pool has reached maximum temperature would permit rapid addition of large amounts of crystalline additive, due to the higher bulk temperatures and higher possible temperatures at the bottom of the pool. The effect of hydrostatic head (pressure) on pool water boiling point, in the case of the Fukushima-Daiichi pools, raises boiling point to 122°C at the bottom of a pool which has been sloshed below 11m depth by seismic action. This effect could also be mitigated by novel delivery of a mixture of preparations, such as a hybrid of a powdered component and hollow cast dissolving nodes of additive, which could float or slowly sink to prevent excessive buildup in the vicinity of the rack inlets.

For BWR fuel assemblies such as those at Fukushima, EPRI research [3] has showed that loss of effective cooling, once pool level has dropped below the top of active fuel level, will first occur for the lowest-power assemblies. This is due to less thermal power being available to drive a two-phase mixture across the cladding of the top of the assemblies and subsequent temperature

excursion. As the addition of large amounts of solute will both increase viscosity and reduce the boiling rate at a given bulk pool temperature, the thermal-hydraulic effects of addition could result in a net disadvantage once an accident progresses to this point. As the intent of the addition is to extend the timeline for this consequence, we assess that the probability of such an event is lower than that of current SFP configurations. Detailed thermal-hydraulic analysis is necessary to determine the expectations for the progression of inventory loss and uncovering, as the geometry and behavior of the pool is complex.

Spent fuel pool supporting systems would require engineering evaluations for suitability in an aqueous environment that contains soluble additives many orders of magnitude higher than the service for which they were designed. The obvious challenges presented by the additive include hydraulic stresses imposed by the higher density of the pumped fluid, increased weight stresses on supporting structures of piping, and the short-term impact of a more corrosive environment.

3.3b Corrosion Concerns

The corrosive effects on the fuel assemblies and pool structures were considered using aqueous Acetic Acid solutions as conservative surrogates for the pool environment [5]. Typical fuel assembly materials, along with typical nuclear metallic materials were considered. The effect on nonmetallic SFP structures (such Boraflex neutron absorbers) was not considered. It should be considered that some materials which are suitable for handling concentrated Acetic Acid are attacked by more dilute solutions. Characterization of the corrosion of SFP structures and fuel assemblies under the exact conditions expected in an accident is necessary to develop this technology.

Zirconium and all zirconium-alloys surveyed exhibit acceptable corrosion rates under all environments except for an aqueous environment of boiling acetic acid [5], combined with saturation of gaseous HCl and Cl₂. This environment does not resemble any expected accident condition.

Nickel-based alloys have demonstrated acceptable resistance to corrosion by acetic acid solutions in the absence of oxidizing ions. In the presence of an air sparge, or addition of high concentrations of cupric ions, Nickel 400 has exhibited corrosion rates which would be unacceptable for long-term maintenance of the acetate solution. Additionally, some Inconels have demonstrated unacceptable corrosion rates when in dilute acetic acid solutions containing additional contaminants. This may not occur in a basic or neutral environment, and it may also not occur in strong acetate solutions. It is possible that all of the nickel-based alloys in use would be suitable for service under accident conditions, but characterization of acetate-driven corrosion of nickel-based alloys specifically requires attention.

400 Series stainless steels are unsuitable for handling of acetic acid solutions. Testing is necessary to determine the susceptibility to acetate corrosion under accident conditions. Type 304 stainless steel is widely used in the storage of concentrated acetic acid, and is also used for the storage and shipment of dilute solutions. Type 316 stainless steel is ubiquitous in the processing of acetic acid and therefore highly unlikely to be unsuitable under any foreseeable pool condition. In the event that the pool is entirely evaporated, a new corrosion mode is presented, but that condition is expected to occur after or concurrent with destruction of fuel cladding by Zirconium-Hydride reaction. Any stainless-steel pool structures remaining are unlikely to serve any safety function at this point.

Carbon and low-alloy steels are unsuitable for acetic acid service. Implementation of an additive system for accident mitigation would likely necessitate replacement of any such materials in the pool. Due to the poor general corrosion characteristics of these steels, their presence is not expected in the wetted volume of the pool.

4. Neutron Absorber Alloy

4.1 Introduction and Motivation

In light of dwindling SFP storage space at nuclear power plants across the United States, the question is raised whether or not more compact storage configurations can be developed that significantly improve space allocation in a conventional SFP. Current SFP designs use neutron poisons in the form of absorber plates to maintain subcritical conditions, and these designs need a certain distance between adjacent fuel bundles such that the absorber plates can fit and be effective. If it is possible to develop an alternative neutron poison in the form of a thin absorber on the surface of individual fuel rods, this may allow for fuel rods and assemblies to be placed closer together while maintaining subcriticality.

There is a concern that such a poison coating could become scraped off in a handling accident or by wear-and-tear of normal operation, so it is desirable to find an alloy that will solder/braze effectively to zircaloy and form a strong bond. The coating should be thick enough to perform effectively as the sole absorber in a SFP but not so thick that it poses a challenge to decay heat removal. These concerns as well as neutron activation behavior are used as evaluation criteria in the search to identify a suitable alloy for use in a condensed SFP.

4.2 Alloy Melting Experiments

4.2a Experimental Equipment

The major equipment used for our brazing experiments consisted of a chemical fume hood, a compact enclosed furnace (Thermolyne 120V muffle furnace) fitted with a digital temperature regulator (EUROTHERM 2116), and an open casting pot (Lee 110V melter

furnace). Pictures of these three major pieces of experimental equipment are collected in **Figure 2** below. Note that a brand-new open casting pot was used for this project to reduce the chance of encountering unwanted contaminant materials during melting procedures.



Figure 2: Chemical hood, furnace, and melting pot used in our experiments (L to R)

4.2b Experiment 1: Cu-Cd

The first melting experiment was set up to wet a Cu-Cd alloy to zircaloy-4 samples. This binary alloy system has a eutectic point at 39 wt.% Cd with a melting temperature of 544 °C. Therefore, a small sample of a 0.5-inch diameter cadmium rod and a strip of copper wire were collected in a ceramic crucible at this particular mass ratio using electronic scales present in our laboratory. The crucible was placed in a small enclosed furnace and the temperature was set to 400 °C to first melt the cadmium. Ideally, the cadmium should have melted around 321 °C, forming a pool around the copper so that the copper would dissolve to form our alloy despite pure copper having a melting point that approaches 1100 °C. However, repeated observations of the sample indicated that the copper wire was not dissolving, so we raised the temperature on our

furnace in hopes of speeding up the dissolution. This process of increasing furnace temperature was repeated until we reached the boiling point of cadmium, at which point we abandoned the experiment. The contents of the crucible were given ample time to cool before inspecting the failed alloy and it was found that excessive oxidation on the copper wire had prevented it from dissolving. **Figure 3** shows the heavily oxidized crucible contents that failed to dissolve (note the coating of Cd crystals on the crucible).



Figure 3: Ceramic crucible containing oxidized cadmium and copper

4.2c Experiment 2: Ag45 Alloy

A second melting experiment was arranged, this time using a premade brazing alloy to simplify the process. This second alloy is comprised of 45% Ag, 15% Cu, 16% Zn, and 24% Cd by weight fraction. According to the manufacturer specifications [6], the alloy should be fully melted at 618 °C. We began by melting a small sample of the alloy in a heated casting pot (typically used for lead) until it formed a shallow pool. Several sticks of zircaloy-4 tubing were quickly dipped into the alloy pool and smeared around in hopes of achieving wetting before the zircaloy oxidized. Due to difficulties in performing the dip before significant oxidation occurred,

we attempted two more methods while we had enough silver alloy remaining. The second approach entailed tipping the casting pot up to make the small alloy pool deeper and more concentrated, and a propane torch was introduced to speed up the alloy heating. Multiple zircaloy tubes were dipped into the resulting alloy pool and collected for further inspection. The final method was a more conventional brazing approach for this alloy. On the final attempts of achieving a wet, a brazing flux was applied to the tips of zircaloy tubes while the alloy was heated with a propane torch above the zircaloy. The braze alloy was dripped and smeared on the zircaloy tube while the tube was rotated so that all of the flux was used. All four zircaloy samples are shown in **Figure 4**. Starting on the left, the first two tubes were dipped when only the melting pot was present. The third tube was dipped into alloy that was heated by the pot and propane torch combined, and the fourth tube represents the attempt to use a brazing flux with heat from the torch.



Figure 4: Zircaloy tubing samples after Ag45 dip application

Upon visual inspection of the zircaloy tubes from the silver alloy experiment, the best sample was determined to have come from the second method. Further inspection under a

microscope indicated that wetting occurred successfully with the melting pot/butane torch combination. The diameter of the best sample was measured to be 9.86-mm after dipping (compared to 9.3-mm original diameter), and the second best sample had a diameter of 9.58-mm. Due to the alloy's tendency to "clot" from uneven heating and oxidation, it is very likely that these diameters are overestimated. For practical purposes, the results indicate that a coating of at least 50- μm is possible. However, both experiments suffered greatly from the effects of oxidation, so further research with these alloys may require the use of an inert atmosphere melting configuration. This may be particularly true if large scale operations are pursued. It is possible that using deeper pools of brazing alloy could mitigate the effects of oxidation as well since the shallow pools were so susceptible to the aforementioned "clotting" problem.

4.3 Criticality Safety Analysis

Several criticality safety evaluations were conducted on the Ag45 brazing alloy within the context of spent fuel pool storage. The SCALE 6.1 software package was used to complete the evaluations with simplified fuel bundle arrangements. Westinghouse 17x17 PWR-type fuel assemblies were used as a template to construct fuel rod and bundle geometries [7], and some key assumptions were made in order to run the software. First, it is assumed that 50- μm of Ag45 alloy is applied uniformly to the clad surface on every single fuel rod in all codes using the absorber alloy. Second, all UO_2 fuel is assumed have an enrichment of 5% U-235 for every single fuel rod. Third, it is assumed that aluminum is an acceptable replacement for zinc for the purpose of evaluating criticality safety. This substitution was made because SCALE 6.1 cross sections libraries do not contain sufficient data for zinc to run an evaluation. Aluminum was chosen specifically because it is rather transparent to neutrons, making it a conservative option.

For comparison, the micro and macroscopic thermal neutron absorption cross sections of zinc are $\sigma_a = 1.10$ b and $\Sigma_a = 0.072$ cm⁻¹ and for aluminum they are $\sigma_a = 0.241$ b and $\Sigma_a = 0.015$ cm⁻¹ [8].

4.3a Standard Spent Fuel Model

The first pool configuration was an attempt to approximate actual spent fuel pools used in industry based on publicly available photographs. 400 PWR-type fuel bundles were arranged in a 20x20 matrix, and they are submerged about 5 meters below the surface of an 11-meter deep pool of pure water. 1 meter of concrete surrounds the bottom and sides of the pool acting as a neutron reflector. Adjacent bundles are spaced 6-cm apart, but no structural dividers or absorber plates are included in the code. **Figure 5** below depicts a vertical and horizontal cutaway of one pool corner. Without the Ag45 alloy coating, the spaced configuration would be supercritical ($k_{\text{eff}} = 1.29$), but with a 50- μm alloy coating present the same layout is subcritical by a wide margin ($k_{\text{eff}} = 0.55$).

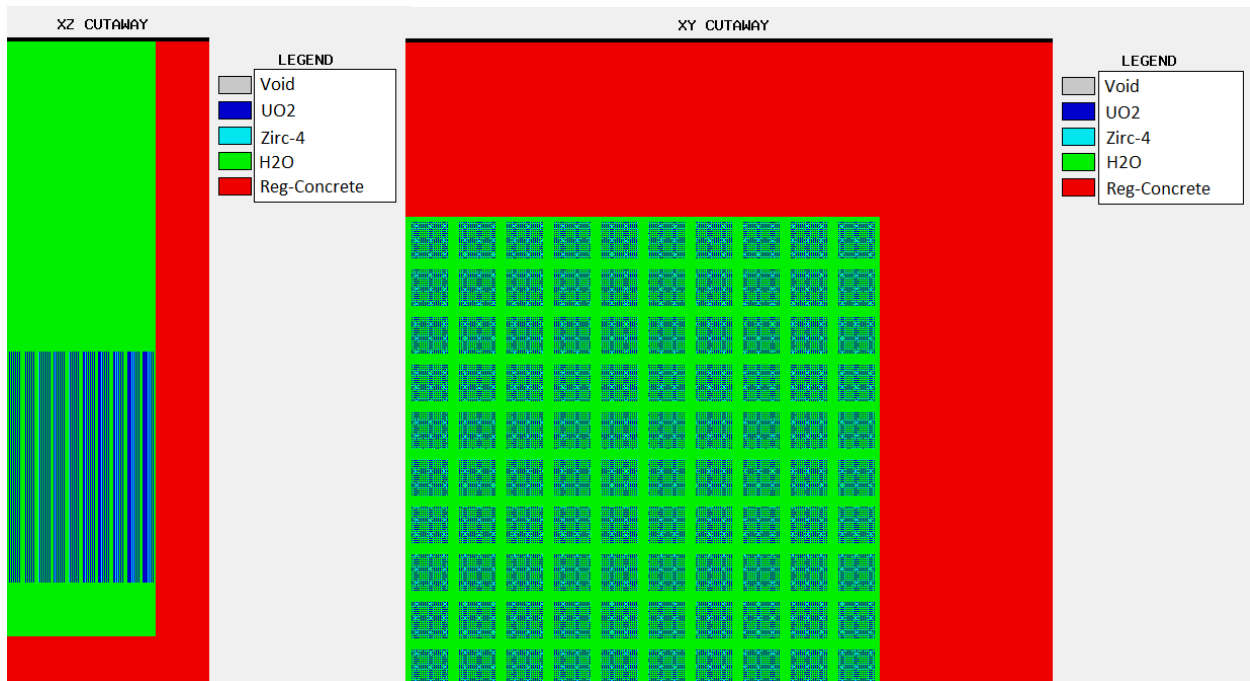


Figure 5: Corner of SFP with 6-mm spacing between bundles

This configuration was also simulated with other alloy thickness to determine a relationship between coating thickness and k_{eff} , and the results of the other simulations are displayed in **Figure 6** below. The red dotted line corresponds to $k_{\text{eff}} = 0.95$ which is frequently used as the maximum allowable k_{eff} in criticality safety evaluations. This plot indicates that a coating thinner than 50- μm could be used to maintain an acceptable margin of subcriticality in our standard SFP configuration, but it is unknown if an industrial-scale dipping process could reliably apply such a thin coating. We suspect it will be difficult to control the alloy application to within such a thin coating based on our own Ag-45 experiment. Therefore, the remaining SFP models will still use the assumption that the coating is 50- μm thick.

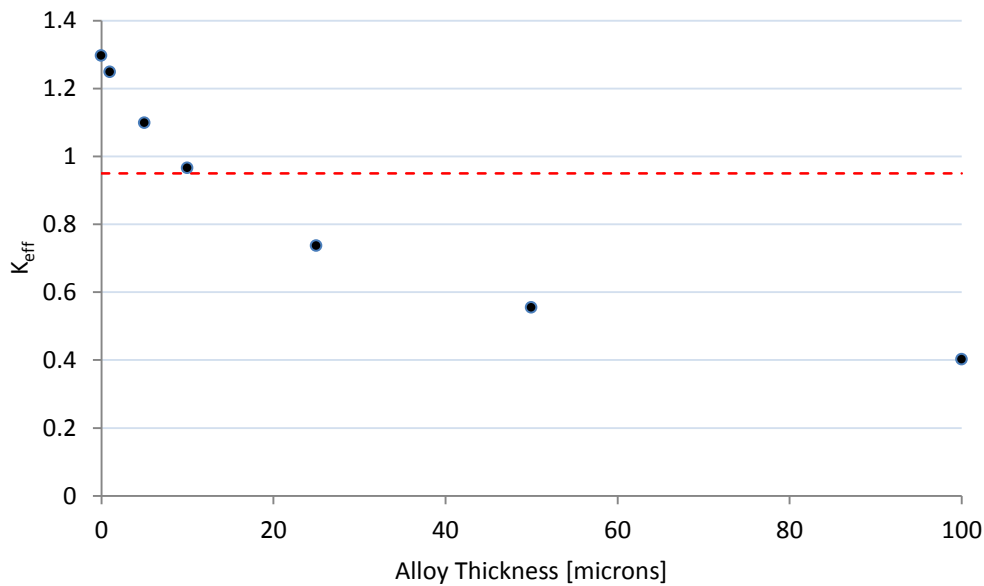


Figure 6: k_{eff} versus Ag-45 coating thickness for a standard SFP

4.3b Spent Fuel Pool with Close-Packed Bundles

The second configuration closely matches the first with one major change: the 6-cm spacing between bundles has been removed. The pool contents were effectively converted to one

giant 340x340 fuel bundle with this modification. This setup was used to test the effectiveness of the Ag45 alloy in the context of severe space limitations for a spent fuel pool. Without any absorber present, the pool was found to be very supercritical ($k_{\text{eff}} = 1.59$). Adding in the uniform alloy coating brought the pool down to subcritical levels ($k_{\text{eff}} = 0.69$), indicating that the alloy can be highly effective in a scenario where fuel bundle arrangements are condensed to the point of touching one another. **Figure 7** below depicts the tightly packed fuel rods in this setup.

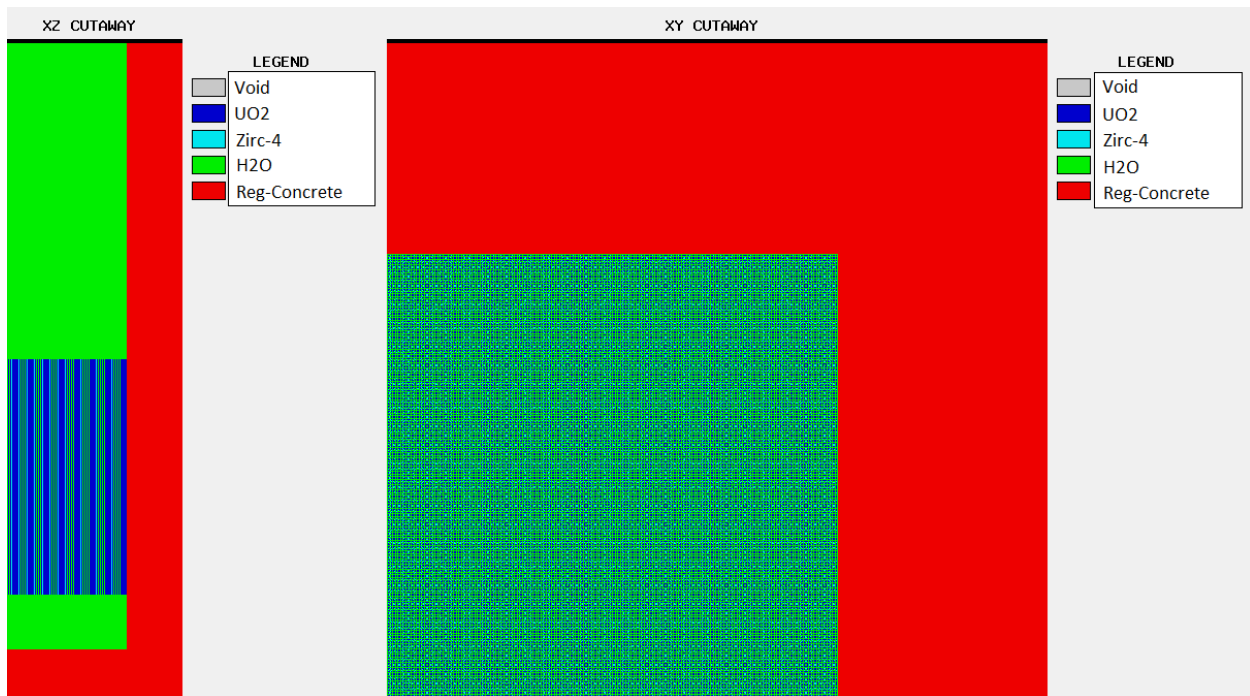


Figure 7: Corner of SFP with minimal bundle spacing

4.3c Spent Fuel Pool with Rod Spacing Removed

The final pool configuration is the most ambitious, and it is intended to model a scenario where fuel rods have been removed from the 17x17 arrays and packed directly together. The rods are still submerged in pure water, and they are assumed to remain in a square lattice arrangement as opposed to a hexagonal lattice. The same pool and concrete format is used, except the pool in

this case is narrower due to the close packing. **Figure 8** shows a close up cutaway view of the assumed lattice, with and without the absorber alloy. The arrangement is supercritical without an absorber ($k_{\text{eff}} = 1.28$) and subcritical with the alloy ($k_{\text{eff}} = 0.79$), indicating that coated fuel rods could be placed extremely close together in a spent fuel pool if thermal characteristics allow it.

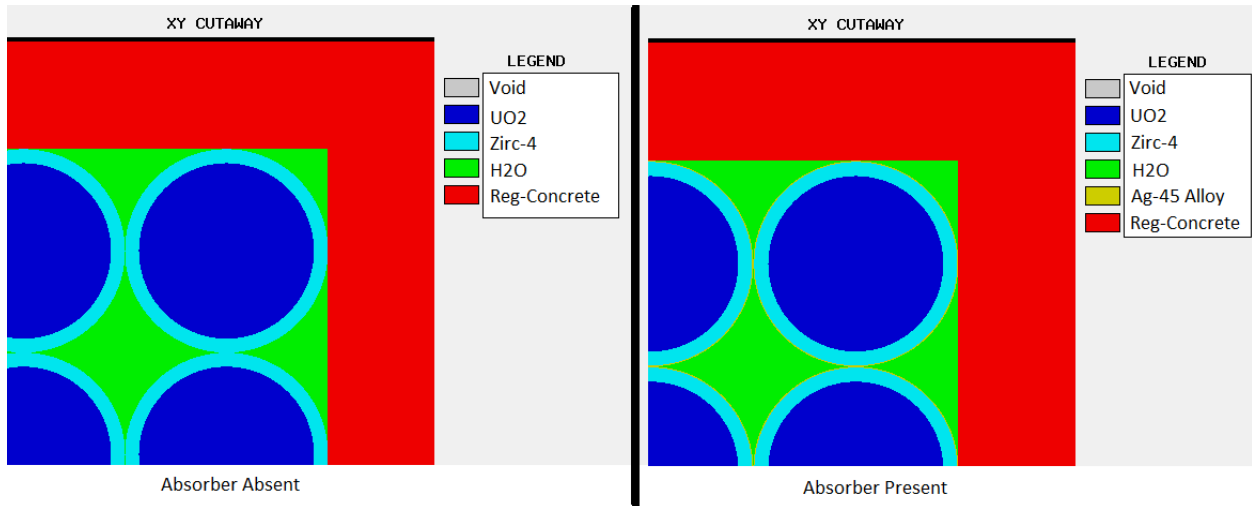


Figure 8: Close-up comparison of tight-packed array with and without Ag45 alloy

4.4 Thermal Analysis

When selecting a suitable neutron poison coating it is important to also consider the thermal impact that the coating will have on the spent nuclear fuel. Heat transfer is already problematic without a coating resulting in the requirement for spent nuclear fuel to spend several years in wet storage before moving to dry storage. In order to thoroughly analyze the impact of a coating on a spent fuel element a computational method should be implied. The impact on the overall thermal performance of the cask could also be determined. However, a thermal code is not available to the research group at this time so an analytical approach is taken. There are several assumptions and generalizations that are made.

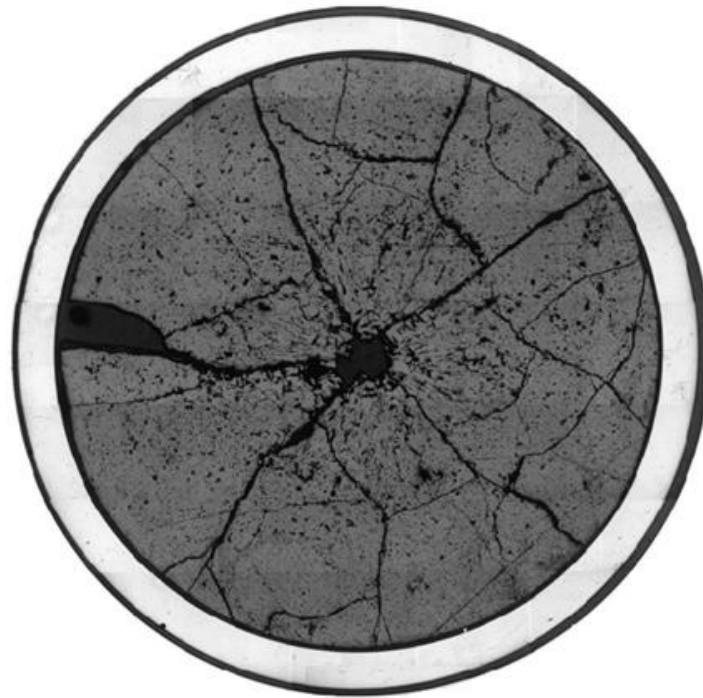
Temperature gradients in the fuel combined with loads determine potential for material failure. The fuel temperature is dependent on a number of factors. In this analysis we do not consider the actual heat transfer. We consider only the thermal resistive network and the resistance of the neutron poison compared to the other materials in the fuel. An initial analysis was performed to determine the contribution of the coating material to the thermal resistance network.

The method for this analysis is outlined in Todreas, Schmidt, and Duderstadt. First, consider the thermal properties of the fuel itself, UO₂. The analysis determines the thermal conductivity of UO₂ at 95% theoretical density. This analysis considers the thermal conductivity estimate formulated by Westinghouse [7].

$$k = \frac{1}{11.8 + 0.0238T} + 8.775 * 10^{-13} * T^3$$

It should be noted that there is a polynomial expansion of the thermal conductivity that is used by Babcock and Wilcox as well as an expansion from Combustion Engineering. The thermal properties are determined by temperature, porosity, oxygen to metal atomic ratio, Plutonium content, pellet cracking, and burnup. There are procedures to determine the contribution of each of these effects to the overall heat transfer. The individual effects are not considered as this analysis is concerned with the macroscopic heat transfer.

It is important to note that there are changes that occur in the fuel as it is burned. Due to high temperatures and irradiation the structure of the fuel may change. If there is a region in the fuel which exceeds a certain threshold, sintering, a loss of porosity may occur. This leads to regions where there is a void at the center with a ring of dense fuel. These changes typically occur within the first few days of operation. **Figure 9** contains a fuel pin cross section showing the combined effects of thermal stress and neutron irradiation on uranium oxide [9].



1mm

Figure 9: Cross section of a fuel pellet after exposure to irradiation and thermal stresses

As a result, it is often necessary to consider temperature distributions across three zones. Due to changes in the material that occur during irradiation is often not appropriate to assume that the fuel has uniform properties. The material changes that are accounted for in a multi zone thermal analysis will reduce the thermal resistance between the centerline and outside pellet. Multi zone heat transfer also accounts for porosity, oxygen to metal atomic ratio, plutonium content, pellet cracking and burnup. However, for the purpose of this analysis, this effect is not considered, and a single zone thermal analysis is conducted.

The next area that is considered is the gap between the fuel pellet and the cladding. This is a space that is usually filled with an inert gas such as helium. The fill gas changes with burnup

due to the release of gaseous fission products. Variations in the gap width arise due to pellet cracking. Thermal expansion of the fuel further reduces this gap. The gap reduction and contact between the pellet and clad reduces thermal resistance. The variation in gap distance is not considered and a mean gap distance is chosen. This value is provided by Todreas [7], and a diagram of these values is included in **Figure 10** below.

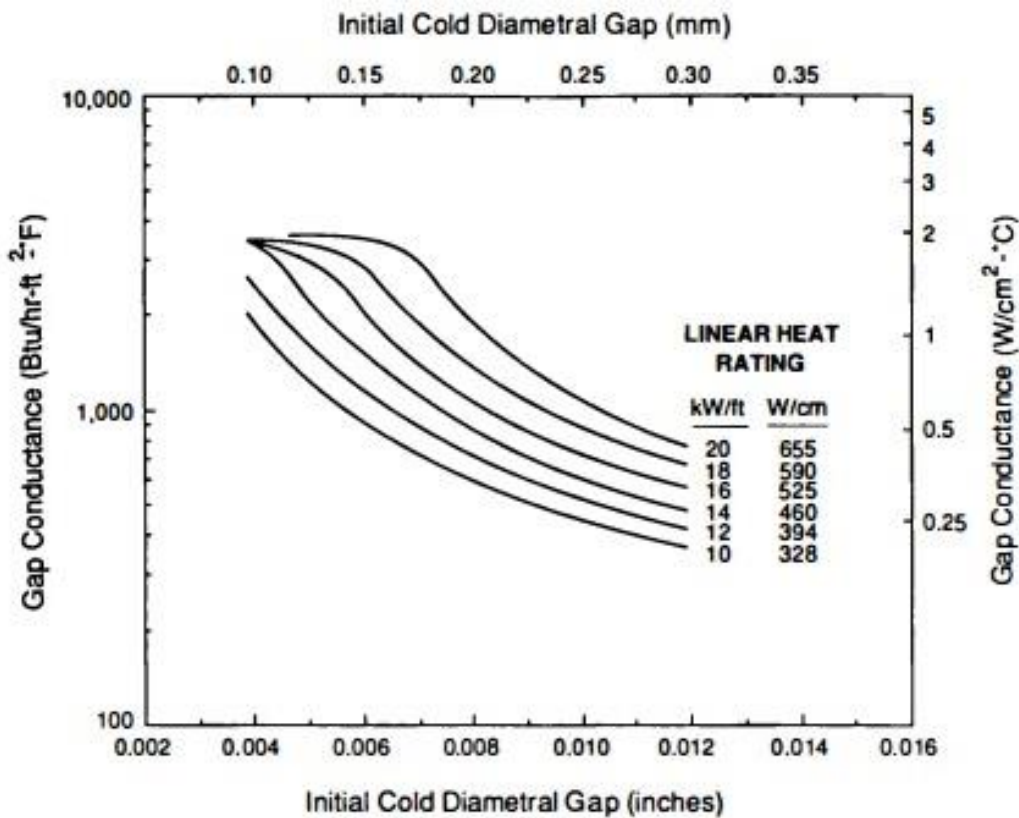


Figure 10: Effect on pellet-to-cladding gap distance on thermal conductivity

The contribution of the coating must also be calculated. Typically, the heat transfer coefficient of many materials is determined experimentally. An estimate of the heat transfer of our alloy was calculated using weighted averages of the component materials. It should be noted that the component of the alloy with the lowest thermal conductivity is still much greater than

that of UO₂. The neutron poison coating was estimated at a thickness of 1mm. The final thermal resistance network is:

$$\Sigma R = \frac{1}{4\pi k_f} + \frac{1}{2\pi R_g h_g} + \frac{\ln\left(\frac{R_{Co}}{R_{Ci}}\right)}{2\pi k_c} + \frac{\ln\left(\frac{R_{Po}}{R_{Ci}}\right)}{2\pi k_p} + \frac{1}{2\pi R_{Po} h_a}$$

The resistance of the coating is orders of magnitude lower than that of UO₂. It can be concluded that the coating will not appreciably hinder the thermal conductivity of the spent fuel. A plot has been included below in **Figure 11** to illustrate the clad temperature vs applied thickness in a range from 0.5-mm to 1.0-cm. The code to generate this plot is attached in the appendix. The code assumed a centerline temperature of 1400 °C and a bulk coolant temperature of 324 °C. The graph further shows how little impact the thermal resistance of the coating has. However, future work using computational codes is needed to verify this result. Additional calculations are provided in the appendix.

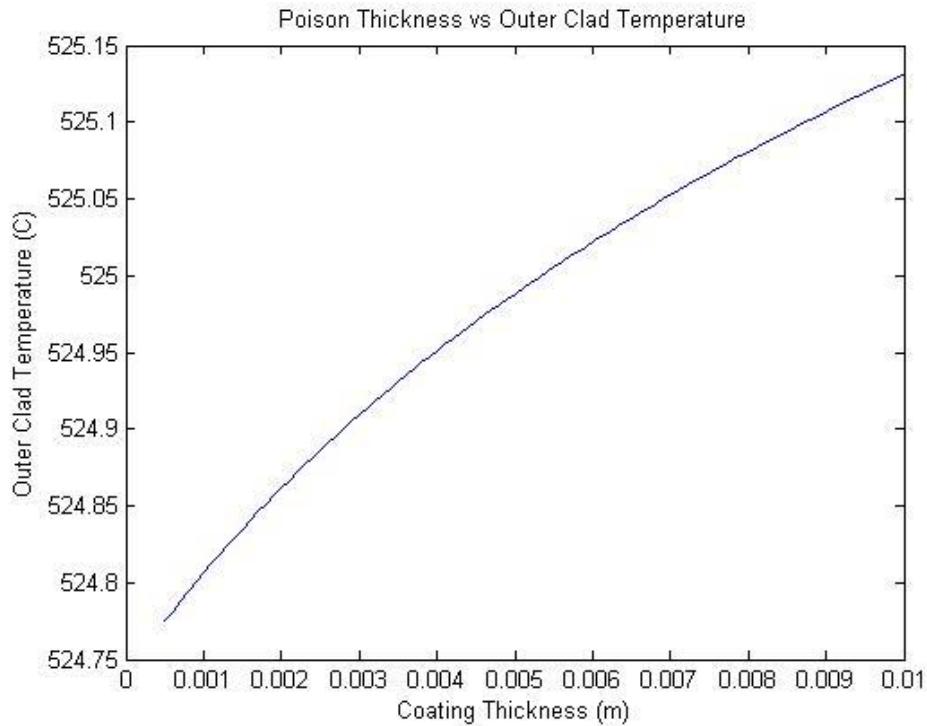


Figure 11: Projected outer fuel-clad temperature as a function of alloy coating thickness

4.5 Neutron Activation Analysis

As part of the consideration for using Silveralloy 45 as the dipping alloy to coat the spent fuel rods, it is necessary to analyze how each component of the alloy will respond to the neutron flux from the spent fuel. Because the manufacturer does not specify the isotopic make-up of each element in the alloy [6], natural abundances have been assumed.

The primary component of the alloy by weight percent is silver at 45%. Natural silver is 51.84% Ag-107 and 48.16% Ag-109. Ag-107 has a thermal neutron absorption cross section of 37 barns and Ag-109 has a cross section of 91 barns. Upon absorption of a neutron, both silver nuclei will decay through beta-minus decay into stable isotopes of cadmium.

The copper weight percent component of Silveralloy 45 is 15%. Similarly to silver, natural copper is composed of two isotopes; 69.15% Cu-63 and 30.85% Cu-65. The thermal neutron absorption cross-section of both isotopes is only a few barns each, however, 4 and 2 barns respectively. With half-lives of only minutes and hours, the copper isotopes decay to stable isotopes of zirconium.

Perhaps the most important component of the alloy is cadmium which is 24% by weight. The neutron absorption characteristics of cadmium were the reason Silveralloy 45 was chosen as a dip initially, with cadmium having a thermal neutron cross section around 2450 barns. The absorption of neutrons by cadmium is the desired effect of the alloy and therefore neutron activation of cadmium is not further considered. The final component zinc, composing 16% of the alloy by weight, does not have any appreciable neutron absorption characteristics.

The two smallest components of the alloy can be generally ignored as zinc does not absorb thermal neutrons and the copper atom ratio is very small in comparison to the very large amounts of cadmium and silver. The large silver component however is significant. Although the

cross-section for silver is quite small compared to the large absorption cross-section of the cadmium, it may seem that the material composition could potentially change due to the transmutation of the large amount of silver. It is currently unknown but this may have negative effects on the performance of the alloy coating. However, due to the relatively low neutron flux in the SFP, about 10^8 neutrons/cm²/sec, the transmutation of silver is not a concern [10]. Even so, if the silver did transmute, the large cross sections of the resulting cadmium isotopes could prolong the effectiveness of the alloy as a neutron absorber.

A rough burnup calculation for the alloy can be made to estimate the time until half of the effective absorber material (namely cadmium) is depleted. For the sake of simplicity, several assumptions are made. First, the neutron flux in the SFP is assumed to be 10^8 neutrons/cm²/sec [10]. Second, all neutrons are assumed to be thermalized by the pool water. Also, cadmium is assumed to be the only active neutron absorber based on the size of its thermal neutron cross section relative to the other elements. Finally, the effects of silver transmutation into cadmium are ignored. An equation for the expected reaction rate is given by the equation:

$$R = -\frac{dN_{Cd}}{dt} = N_{Cd}\sigma_a\phi$$

where N_{Cd} is used to represent the remaining amount of cadmium absorber. A general solution for the differential equation is:

$$N_{Cd} = Ke^{-\sigma_a\phi t}$$

where K is a boundary condition. The half-life for this general solution can easily be determined without the need for a given boundary condition using the expression

$$t_{half-life} = \frac{\ln\{2\}}{\sigma_a\phi} = \frac{\ln\{2\}}{(2450 b)(10^8 cm^{-2}s^{-1})} = 2.83 \times 10^{12}s \cong 90,000 y$$

A half-life of 90,000 years indicates that absorber burnup will be insignificant for the duration of SFP storage at the assumed flux levels. In the unlikely event that the coated rods were reintroduced to a high flux environment (such as in a criticality accident) this time could be greatly reduced. However, it is inferred from our criticality safety analysis that a SFP using our absorber will remain subcritical by a wide margin.

5. Conclusions

5.1 Spent Fuel Pool Additive

The addition of a soluble additive to the SFP of a damaged reactor facility can potentially extend the grace period of important events and consequently reduce the probability of serious releases of the fission products contained in stored fuel assemblies. The additive considered, sodium acetate, appears to present a low corrosion hazard to the fuel assemblies, pool structures, and pool liner. Additionally, exposure of concrete to the SFP water would reduce concrete permeability. Sodium acetate does not present a toxic hazard to plant personnel or the environment. The corrosion rates exhibited by test specimens in the literature are acceptable over the short timespan that the additive is expected to be present in the pool. The increased viscosity and boiling point of the pool water could serve to lower the probability of a severe pool accident, but detailed thermal-hydraulic analyses are necessary to verify that addition will not excessively exacerbate the progress of an accident once the pool inventory has dropped below the top of active fuel, as vigorous boiling and two-phase flow serves to cool fuel elements. Corrosion testing of the exact materials used in pools, across the range of normal and accident conditions, will also be necessary to safely implement this technology.

5.2 Neutron Absorber Alloy

Applying a neutron absorbing alloy to the clad surface of spent nuclear fuel rods can be very effective in preventing a criticality excursion within a SFP environment. Multiple SCALE models were created to test the safety performance of a commercially available Ag45 Silveralloy (containing 24% cadmium by weight) and the alloy provided yielded high margins of safety in

each case. Every storage configuration was tested twice, once without any neutron absorbers and once with a 50- μm coating of the alloy on all fuel rods, and the alloy consistently proved to be capable of maintaining sub-criticality with no assistance from absorber plates typically used in SFPs. In the model representative of a standard SFP, k_{eff} was brought down from 1.29 to 0.55 by the alloy. In a similar SFP with fuel bundles placed very close together, the alloy took k_{eff} from 1.59 down to 0.69. A final model was prepared to represent a scenario where individual fuel rods were removed from the fuel bundles and placed directly against one another in a square pitch geometry, and the alloy reduced k_{eff} from 1.28 to 0.79. Results from the latter two scenarios demonstrate that the alloy could be useful for storage situations designed to maximize fuel storage in a limited space.

A thermal analysis for the Ag45 alloy coating indicates that the alloy coating would contribute a minor amount to thermal resistivity to the fuel rods when compared to the resistivity from the UO_2 fuel pellets. A simulation was conducted to determine the relationship between alloy coating thickness and outside clad temperature, and the simulation indicates that outside clad temperature would increase minimally even for very thick coatings on the order of several millimeters. Since the criticality safety analysis showed that coatings much thinner than 1-mm are sufficient for maintaining sub-criticality, it is unlikely that such thick coatings would be used in practice where cost-saving measures are crucial. A more in-depth analysis with specialized software is necessary to confirm these results before this design can truly be considered viable.

Neutron activation analysis on the Ag45 alloy does not suggest that any particularly troublesome isotopes would be produced in a SFP environment. However, the analysis did suggest that activated silver in the alloy may undergo beta decay transmutation into more cadmium. Considering that cadmium is the desired absorber element, and that silver comprises

the largest fraction of the alloy by weight, this suggests that the effective lifespan of the alloy would be longer than anticipated if only the original cadmium was used in burnup estimations. This is generally not a great concern for basic fuel storage where the neutron flux is significantly lower than a reactor setting. A simple burnup estimation using for typical SFP flux conditions indicated that the cadmium burnup will be negligible for the duration of pool storage.

6. Future Work

The extent of practical applications and methods discovered in only one semester spent on this major design project is obviously limited. A vast amount of research and design must still be done before our ideas could be put into real world practice. In multi-billion dollar facilities, every new change to the system must be perfectly designed and regulated.

6.1 Additive Concerns

While the spent fuel pool additive may allow for a needed extended grace period during an emergency, it may also have some negative effects that require further testing. When added while the SFP is at a cooler temperature, the additive could potentially hinder cooling water flow through fuel assemblies. Tests must be done to determine whether the additive can be added while the SFP is at normal temperatures or after the temperature has increased to a level where the additive can completely dissolve in the water upon addition. Additional thermal-hydraulic analysis is required to determine expectations for how the water would react once the water began to boil and potentially uncover the fuel. Any plant that actually implemented our sodium acetate additive would have to remove all stainless steel and alloy steel materials in the fuel pool to prevent corrosion.

The raw material cost for sodium acetate varies depending on quality and quantity, with smaller 500g laboratory-oriented samples costing \$20 to \$30 per kilogram [11]. However, significantly lower unit prices are possible if purchased in bulk. The exact price per pool would depend on pool size and additive concentration. Future work is recommended to determine the

concentration and price to treat a SFP with this additive, including whether or not new filtration, ion exchange, or cooling systems must be developed to handle the additive.

6.2 Thermal Analysis

It is recommended that a full thermal-hydraulic code is used to analyze the impact of the neutron absorber alloy on thermal resistance of the system. The analysis used did not consider cracks or changes in porosity, both of which are common occurrences. Additionally, the total impact of the coating is not known. While contribution to the thermal resistance for one rod is known, it is unknown what effect this will have on the heat transfer of the cask. The system is too complex to simply extrapolate the additional resistance to heat transfer by multiplying the resistance times the number of rods. It is possible that a more in-depth analysis would show that this coating would not be feasible given the current limitations of heat transfer inside a dry cask. The code should also be leveraged to determine the effect on the bulk temperature of the water in the spent fuel pool. It is possible that this resistance, although low, would have significant impact on the spent fuel pool.

6.3 Economic Viability and Retrofit Potential

The absorber alloy analysis does not consider the cost either in time or money for such an operation. Economically, several problems arise immediately. The first is the sheer cost of the alloy itself. An alloy that is 45% silver by weight is expensive. The process of coating the fuel will also prove costly. It is likely that an inert atmosphere will have to be used to prevent the oxidation of zircaloy at the temperatures at which the alloy is applied. It is possible that the rods may be removed from the assemblies and coated individually leading to a smaller processing

area, but this may be more costly than dipping the entire assembly. A rough estimate for solely the material cost of a 50- μm Ag-45 coating per rod would be 58 grams (6.4 cm^3 of alloy) at \$1.53/gram (\$43.33/ounce [10]), or around \$89 a rod. This translates to around \$25,700 per 17x17 fuel assembly for just the Ag-45 alloy alone. Further work is recommended to determine the total cost of dipping complete with transportation, handling, and other associated prices.

The equipment to perform these operations does not exist on site. Transporting the spent fuel off site is not very likely unless it is headed for a repository. Therefore, the work must be done on site in a newly fabricated facility. Since our group had a very limited supply of the alloy to use in experimental dip coatings, the dipping process is still relatively unknown and inconsistent. A consistent dipping process must be determined to ensure quality coatings on all fuel assemblies dipped in the new process. Even though the Ag-Cd-Cu-Zn alloy was able to wet a zirconium rod in our laboratory, extensive tests and trial runs must be performed to determine the feasibility of actually implementing this dip process. Also, it is imperative to find a way to safely shield the working environment from the radiation given off by fuel assemblies removed from the pool to be coated. One potential idea is a large concrete tube to pull the used fuel assembly into as it is being removed from the SFP. Further work is recommended to determine the industrial process to properly handle and coat these assemblies.

7. References

1. NEI Fact Sheet: Status of Used Nuclear Fuel Storage at U.S. Commercial Nuclear Plants. February 2009.
2. United States Nuclear Regulatory Commission. NUREG-1536 Standard Review Plan for Dry Cask Storage Systems. January 1997. pp. 4-1.
3. Summary of the EPRI Early Event Analysis of the Fukushima Daiichi Spent Fuel Pools Following the March 11, 2011 Earthquake and Tsunami in Japan. EPRI, Palo Alto, CA: 2012. 1025058.
4. Al-Otoom, Awni, Abdelaziz Al-Khlaifa, and Ahmed Shawaqfeh. "Crystallization Technology for Reducing Water Permeability into Concrete." *Industrial & Engineering Chemistry Research* 46.16 (2007): 5463-467.
5. Craig, Bruce D. *Handbook of Corrosion Data*. Materials Park, OH: ASM International, 1995.
6. "Silveraloy 45 (SA45) Technical Data." The Prince & Izant Company. Accessed via web.
7. Todreas, Neil E. and Mujid S. Kazimi. *Nuclear Systems Volume 1: Thermal Hydraulic Fundamentals*, 2nd Ed. Boca Raton: Taylor & Francis, 2012. Print.
8. Duderstadt, James J. and Louis J. Hamilton. *Nuclear Reactor Analysis*. New York: Wiley, 1976. Print.
9. Tanaka, K. et al. Microstructure and Elemental Distribution of Americium-Containing Uranium Plutonium Mixed Oxide Fuel under a Short-Term Irradiation Test in a Fast Reactor, *Journal of Nuclear Materials*, vol.385, issue 2, 2009, p.407-412.

10. Grossbeck, Martin L. Private communication. 22 Apr 2014.
11. Carolina Biological Supply Company. Sodium Acetate, anhydrous, laboratory grade, 500g. Accessed via web. <<http://www.carolina.com/>>.

Appendix A: SCALE 6.1 Models

Spent fuel pool with no additional absorber:

```
=csas25 parm=(nitawl)
Spent Fuel Pool without Absorber Alloy
44groupndf5
read composition
uo2      1 DEN=9.21 1.00      300 92235 5 92238 95 end
zirc4    2          1.00      300                    end
h2o      3          1.00      300                    end
reg-concrete 5          1.00      300                    end
end composition
read param
gen=203 npg=1000 nsk=3
end param
read geometry
unit 1
  cylinder 1 1 0.4095 426.7 0
  cylinder 2 1 0.4750 426.7 0
  cuboid 3 1 0.63 -0.63 0.63 -0.63 1000 -100
unit 2
  array 1 -10.71 -10.71 -100
  cuboid 3 1 4p13.71 1000 -100
global unit 3
  array 2 -274.2 -274.2 -100
  cuboid 5 1 4p374.2 1000 -200
end geometry
read array
ara=1 nux=17 nuy=17 nuz=1 fill f1 end fill
ara=2 nux=20 nuy=20 nuz=1 fill f2 end fill
end array
read plot
scr=yes
ttl='xz cutaway'
pic=mixtures
xul=0
yul=3.63
zul=1000
xlr=374.2
ylr=3.63
zlr=-200
nax=200
ndn=640
uax=1 vax=0 wax=0
udn=0 vdn=0 wdn=-1
end
scr=yes
ttl='xy cutaway'
pic=mixtures
xul=0
yul=374.2
zul=0
xlr=374.2
ylr=0
zlr=0
nax=640
ndn=640
uax=1 vax=0 wax=0
udn=0 vdn=-1 wdn=0
end
end plot
end data
end
```

Spent fuel pool with all rods coated in Ag45 absorber alloy:

```
=csas25 parm=(nitawl)
Spent Fuel Pool with Absorber Alloy
44groupndf5
read composition
uo2      1 DEN=9.21 1.00    300 92235 5 92238 95 end
zirc4    2          1.00    300          end
h2o      3          1.00    300          end
ag        4          0.39071          end
cu        4          0.15248          end
al        4          0.20410          end
cd        4          0.25271          end
reg-concrete 5      1.00    300          end
end composition
read param
gen=203 npg=1000 nsk=3
end param
read geometry
unit 1
cylinder 1 1 0.4095 426.7 0
cylinder 2 1 0.4750 426.7 0
cylinder 4 1 0.4800 426.7 0
cuboid   3 1 0.63 -0.63 0.63 -0.63 1000 -100
unit 2
array 1 -10.71 -10.71 -100
cuboid 3 1 4p13.71 1000 -100
global unit 3
array 2 -274.2 -274.2 -100
cuboid 5 1 4p374.2 1000 -200
end geometry
read array
ara=1 nux=17 nuy=17 nuz=1 fill f1 end fill
ara=2 nux=20 nuy=20 nuz=1 fill f2 end fill
end array
end data
end
```

Condensed spent fuel pool with no absorber alloy:

```
=csas25 parm=(nitawl)
Spent Fuel Pool without Absorber Alloy **CONDENSED**
44groupndf5
read composition
uo2      1 DEN=9.21 1.00      300 92235 5 92238 95 end
zirc4    2          1.00      300          end
h2o      3          1.00      300          end
reg-concrete 5      1.00      300          end
end composition
read param
gen=203 npg=1000 nsk=3
end param
read geometry
unit 1
cylinder 1 1 0.4095 426.7 0
cylinder 2 1 0.4750 426.7 0
cuboid 3 1 0.63 -0.63 0.63 -0.63 1000 -100
unit 2
array 1 -10.71 -10.71 -100
cuboid 3 1 4p10.71 1000 -100
global unit 3
array 2 -214.2 -214.2 -100
cuboid 5 1 4p314.2 1000 -200
end geometry
read array
ara=1 nux=17 nuy=17 nuz=1 fill f1 end fill
ara=2 nux=20 nuy=20 nuz=1 fill f2 end fill
end array
read plot
scr=yes
ttl='xz cutaway'
pic=mixtures
xul=0
yul=0.63
zul=1000
xlr=314.2
ylr=0.63
zlr=-200
nax=170
ndn=640
uax=1 vax=0 wax=0
udn=0 vdn=0 wdn=-1
end
scr=yes
ttl='xy cutaway'
pic=mixtures
xul=0
yul=314.2
zul=0
xlr=314.2
ylr=0
zlr=0
nax=640
ndn=640
uax=1 vax=0 wax=0
udn=0 vdn=-1 wdn=0
end
end plot
end data
end
```

Condensed spent fuel pool with Ag45 alloy present on all rods:

```
=csas25 parm=(nitawl)
Spent Fuel Pool with Absorber Alloy **CONDENSED**
44groupndf5
read composition
uo2      1 DEN=9.21 1.00    300 92235 5 92238 95 end
zirc4    2          1.00    300          end
h2o      3          1.00    300          end
ag       4          0.39071          end
cu       4          0.15248          end
al       4          0.20410          end
cd       4          0.25271          end
reg-concrete 5      1.00    300          end
end composition
read param
gen=203 npg=1000 nsk=3
end param
read geometry
unit 1
cylinder 1 1 0.4095 426.7 0
cylinder 2 1 0.4750 426.7 0
cylinder 4 1 0.4800 426.7 0
cuboid 3 1 0.63 -0.63 0.63 -0.63 1000 -100
unit 2
array 1 -10.71 -10.71 -100
cuboid 3 1 4p10.71 1000 -100
global unit 3
array 2 -214.2 -214.2 -100
cuboid 5 1 4p314.2 1000 -200
end geometry
read array
ara=1 nux=17 nuy=17 nuz=1 fill f1 end fill
ara=2 nux=20 nuy=20 nuz=1 fill f2 end fill
end array
end data
end
```

Spent fuel pool with rods removed from 17x17 arrays and pressed together in a square pitch;
absorber not used:

```
=csas25 parm=(nitawl)
Spent Fuel Pool with Absorber Alloy
44groupndf5
read composition
uo2      1 DEN=9.21 1.00    300 92235 5 92238 95 end
zirc4    2          1.00    300          end
h2o      3          1.00    300          end
ag       4          0.39071          end
cu       4          0.15248          end
al       4          0.20410          end
cd       4          0.25271          end
reg-concrete 5          1.00    300          end
end composition
read param
gen=203 npg=1000 nsk=3
end param
read geometry
unit 1
  cylinder 1 1 0.4095 426.7 0
  cylinder 2 1 0.4750 426.7 0
  cuboid 3 1 0.475 -0.475 0.475 -0.475 1000 -100
unit 2
  array 1 -8.075 -8.075 -100
  cuboid 3 1 4p8.075 1000 -100
global unit 3
  array 2 -161.5 -161.5 -100
  cuboid 5 1 4p261.5 1000 -200
end geometry
read array
ara=1 nux=17 nuy=17 nuz=1 fill f1 end fill
ara=2 nux=20 nuy=20 nuz=1 fill f2 end fill
end array
read plot
scr=yes
ttl='xy cutaway'
pic=mixtures
xul=160
yul=162
zul=0
xlr=162
ylr=160
zlr=0
nax=400
ndn=400
uax=1 vax=0 wax=0
udn=0 vdn=-1 wdn=0
end
end plot
end data
end
```


Spent fuel pool with rods removed from 17x17 arrays and pressed together in a square pitch;
Ag45 absorber alloy present on all rods:

```
=csas25 parm=(nitawl)
Spent Fuel Pool with Absorber Alloy
44groupndf5
read composition
uo2      1 DEN=9.21 1.00    300 92235 5 92238 95 end
zirc4    2          1.00    300          end
h2o      3          1.00    300          end
ag        4          0.39071          end
cu        4          0.15248          end
al        4          0.20410          end
cd        4          0.25271          end
reg-concrete 5          1.00    300          end
end composition
read param
gen=203 npg=1000 nsk=3
end param
read geometry
unit 1
  cylinder 1 1 0.4095 426.7 0
  cylinder 2 1 0.4750 426.7 0
  cylinder 4 1 0.4800 426.7 0
  cuboid 3 1 0.48 -0.48 0.48 -0.48 1000 -100
unit 2
  array 1 -8.16 -8.16 -100
  cuboid 3 1 4p8.16 1000 -100
global unit 3
  array 2 -163.2 -163.2 -100
  cuboid 5 1 4p263.2 1000 -200
end geometry
read array
ara=1 nux=17 nuy=17 nuz=1 fill f1 end fill
ara=2 nux=20 nuy=20 nuz=1 fill f2 end fill
end array
read plot
scr=yes
ttl='xy cutaway'
pic=mixtures
xul=161.75
yul=163.75
zul=0
xlr=163.75
ylr=161.75
zlr=0
nax=400
ndn=400
uax=1 vax=0 wax=0
udn=0 vdn=-1 wdn=0
end
end plot
end data
end
```

Appendix B: MATLAB Thermal Modeling Code

```
_t=.5*10^-3;
n=1;

while n<97

%Variables
R_co=4.75*10^-3; %Radius to clad outer (m)
R_ci=4.18*10^-3; %Radius to clad inner (m)
R_po=R_co+P_t; %Radius to poison outer (m)
Tcool=324; %Temperature of coolant (C)
Tcl=1400; %Fuel CL Temp (C)
rs_to_Tco=.151+.797+.190; %Thermal Resistance to Clad Outer
rs_pos_outer_to_mean=0.261; %Thermal Resistance from Poison Outer to Bulk
rs_Tco_to_pos_outer=log(R_po/R_co)/(2*pi*289); %Thermal Resistance from Clad Outer
%To Poison Outer

%Calculations
SumR=rs_to_Tco+rs_pos_outer_to_mean+rs_Tco_to_pos_outer;
Q=(Tcl-Tcool)/SumR;

TcladOuter=(Q*(.261+rs_Tco_to_pos_outer)+Tcool);

TCoAr(n)=TcladOuter;
ThicknessArray(n)=P_t;
n=n+1;
P_t=P_t+1*10^-4;

end

plot(ThicknessArray,TCoAr)
```